A MODEL-BASED APPROACH TO HYPERSPECTRAL ANALYSIS OF WATER CONSTITUENTS

By
Rolando Raqueño, Rochester Institute of Technology[1]
Rulon E. Simmons, Eastman Kodak Company
Ronald Fairbanks, United States Air Force
John R. Schott, Rochester Institute of Technology

1   INTRODUCTION AND SUMMARY

This paper stems from a NASA EOCAP project for evaluating water quality monitoring with a hyperspectral system. It was worked jointly by the Eastman Kodak Company (prime) and the Rochester Institute of Technology (RIT). Kodak was primarily responsible for surveying the needs of the water quality community and determining hyperspectral system requirements to meet those needs. RIT integrated the models and developed algorithms that are being used to test the capability of monitoring specific water constituents.

A major thrust of this effort was the development and testing of improved algorithms for measuring and mapping the major constituents in optically-complex waters when viewed through a complex atmosphere. An end-to-end model, called HydroMod, was assembled as part of this effort. The model draws together components from various other models and includes some new features. HydroMod mates two established premier codes, MODTRAN and HYDROLIGHT (with enhancements), using an IDL widget-driven interface and consists of four main modules. These modules calculate: (1) input radiance distribution; (2) transitions through the air/water interface; (3) propagation and reflection underwater; and (4) propagation back through the atmosphere to the sensor. Each module emphasizes realistic environmental conditions and accuracy. The ability to insert multivariate clouds in the atmosphere at select locations is also included. HydroMod can effectively be used to study light distributions within the water body, above the water surface and reaching remote sensing platforms orbiting the earth. The HydroMod tool is desribed in more detail by Fairbanks et al. 1999 and will be briefly reviewed here.

In order to take full advantage of the forward propagating HydroMod code, a method for inverting apparent reflectance to multi-parameter in-water constituents was developed. This method uses a non-linear least squares optimization method that iteratively matches observed spectra to spectra predicted by the forward propagating models (both HydroMod and results from Bukata et al. 1995) were tested. This inversion process requires that the modeled and image data be in common radiometric units (typically apparent surface reflectance). To accomplish this, several methods of radiometric normalization/calibration are being considered, one of which will be presented in this paper.

The primary data set being used on this study was acquired on May 20, 1999, including an AVIRIS flight over Lake Ontario. RIT's MISI hyperspectral sensor underflew AVIRIS, providing additional data with higher spatial resolution. A large support team collected water data from the lake and surrounding ponds. This paper focuses on the water quality inversion approach and very early results as applied to AVIRIS data. Because of the recent availability of the Lake Ontario data only very preliminary results on this data set are presented here. Some initial testing of the approach was performed on August 1997 AVIRIS imagery of Narragansett Bay. However, because no surface truth was available, this assessment focused only on general trends in the data.

2   MODELING

A major goal of our modeling effort is to develop and refine tools for extracting water quality parameters from remotely-sensed hyperspectral imagery. This approach uses the water radiative transfer model called HydroMod (a

---

[1] rolando@cis.rit.edu
rulon.simmons@kodak.com
schott@cis.rit.edu
rrf1512@rit.edu

mating of the MODTRAN atmospheric propagation model (cf. Berk 1989) and the HYDROLIGHT water radiance propagation model (cf. Mobley 1994)). The idea is to simulate the water-leaving spectral radiance above and below the surface for varying inputs of water quality parameters. Image-derived spectral measurements can then be compared with this family of predicted water-leaving spectral radiance vectors to find a best match and subsequently the associated water quality parameters that were used to generate the matching vector. This curve fitting approach has been used successfully in the atmospheric compensation regime where iterative MODTRAN runs have been used to derive atmospheric parameters to match remotely-sensed land target spectra (cf. Green et al. 1993 and Sanders et al. 1999). The technique promises to have similar applicability to the water quality problem.

It should be noted that the scope of the modeling analysis has been limited to the water-leaving radiance in the vicinity of the surface instead of the radiance reaching the sensor. This is intended to make the problem more tractable by limiting the degrees of freedom by removing the errors introduced by atmospheric effects from the equation. This can be done when ground truth data or good water truth estimates are available using a model-based empirical line method (ELM). Once the modeling technique using HydroMod has been refined, the atmospheric correction problem over water can be addressed with greater probability of success and fewer sources of uncertainty.

2.1   HydroMod

HydroMod is a computer-aided design tool for studying the remote sensing of water quality parameters. Fundamentally, we seek to solve the forward radiative transfer equations in a realistic environment starting from the sun and ending at the remote sensing platform. Operationally, HydroMod uses two industry standard models to actually solve the radiative transfer equations (MODTRAN and HYDROLIGHT). In that sense, HydroMod is an IDL graphical user interface shell that sets up the "realistic" environment under study. The ability to add clouds into our environment has been added outside of the MODTRAN and HYDROLIGHT pre-existing codes as have several data analysis capabilities. Because both MODTRAN and HYDROLIGHT are standard codes, we will only briefly summarize them here and emphasize the changes included as part of the combined HydroMod tool and the use of HydroMod in the generation of data for the inversion process.

Figure 1 pictorially explains HydroMod. HydroMod simultaneously predicts the radiance in all directions (upward and/or downward hemispheres) using an input set of information for the atmosphere, clouds, wind speed, water, and wavelength bands of interest. The "radiance in all directions" is at the water surface (above and below the surface); at the sensor; at the bottom of the water; and at any specified point within the water body.
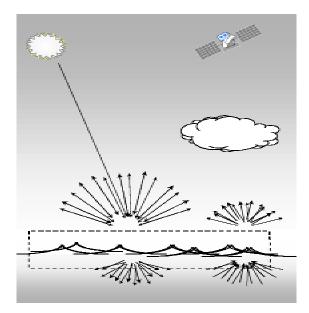

Figure 1: A pictorial representation of a HydroMod radiative transfer scene.

HydroMod uses and computes radiance values into and out the water for all directions in the hemispheres above and below the water. A radiance value is represented by something like $^+L_\lambda^\downarrow(\theta,\phi)$ which represents the spectral (λ) radiance (L) above the water surface (+) heading down ($\downarrow$) from the (θ,ϕ) direction. Sometimes the vertical point in space or within the water column is also designated as in $^-L_\lambda^\uparrow(z;\theta,\phi)$. This represents the spectral radiance below the water surface heading up at a depth of z in the (θ,ϕ) direction. This ability to generate radiance or apparent reflectance estimates within the water column, as well as just above and below the surface is particularly useful because these values correspond to the measurements taken in situ as part of the field collection program.

The first set of radiance values that HydroMod needs is the input sun and sky radiance, $^+L_\lambda^\downarrow(\theta,\phi)$, for the hemisphere above the water surface. HydroMod does this by *either* finding the set of $^+L_\lambda^\downarrow(\theta,\phi)$ values already existing in a lookup table or by iteratively running MODTRAN to generate the $^+L_\lambda^\downarrow(\theta,\phi)$ values needed. The spectral range on all of the LUTs and all of the $^+L_\lambda^\downarrow(\theta,\phi)$ to this point runs from 290nm to 1000nm in 1nm steps.

HydroMod allows for adding clouds to the input hemispherical spectral radiance, $^+L_\lambda^\downarrow(\theta,\phi)$, at the desired ($\theta',\phi'$) directions. These clouds will have a spectral character of their own. They will also have an associated brightness level, and a given quad may be partially sky and partially cloud so that a cloud to cloud plus sky ratio is also needed. HydroMod allows all of these to vary at the users' discretion. It then replaces the radiance from the sky in the (θ',ϕ') direction with the radiance from the user-defined cloud in the (θ',ϕ') direction.

At this point, HydroMod hands off the data to a modified version of HYDROLIGHT. (HYDROLIGHT was created by Dr. Curtis Mobley. For a discussion of HYDROLIGHT and the calculations that it makes, see Mobley 1994, 1995, and 1996). Essentially, it performs the radiance transfer through the wind-roughened water surface, into and within water, and back out of the wind-roughened surface. The numerically-defined wind-roughened surface and the water parameters are key HydroMod inputs. Several wind-roughened surfaces have been generated and are normally included as LUTs with the code. They are for wind speeds of 0 m/sec to 12.5m/sec in 0.5m/sec steps and for the default wind speeds built into MODTRAN (4.1m/sec, 10.3m/sec, 6.7m/sec,…) for the different atmospheric models. These data sets were generated using the probability density functions for surface wave orientations derived by Cox and Munk (1956). HydroMod can calculate the total radiance at the sensor by multiplying the correct transmission coefficients (obtained, again, from either MODTRAN or from one of the LUTs) by the sum of the radiance leaving the water and the radiance reflected off of the water's surface, and then adding in the upwelled radiance. The key input parameters are the solar location, characteristics of the atmosphere, location and spectral character of the clouds in the atmosphere and the concentration and spectral character of water contaminants. However, for the early stages of this study, we are only using HydroMod to generate the surface spectral radiance/reflectance values. We have also assumed clear sky conditions so we will ignore the cloud component of HydroMod. However, we believe this will be one of the most important elements in operational cases where clouds are common.

In addition to the water surface wave formulations from Cox and Munk (1956) and the water index of refraction variability (Quan and Fry, 1995), the key HYDROLIGHT input parameters for water consist of the inherent optical properties (IOP's) of the constituents of interest. These consist of the absorption and scattering coefficients of four primary coloring parameters: pure water, suspended matter (SM- sometimes referred to as total suspended solids); colored dissolved organic matter (CDOM); and chlorophyll-a. (cf. Bukata, 1995). The total absorption and scattering coefficient for the water in question can be determined using EQ. 1 which shows the four parameters of natural waters broken into concentration levels (C_{xx}) and absorption (a) and scattering (b) cross sections. (Note that CDOM does not scatter appreciably and b_{CDOM} is assumed to be zero.)

$$a(\lambda) = a_{water}(\lambda) + C_{CDOM}\,a_{CDOM}(\lambda) +$$
$$C_{SM}\,a_{SM}(\lambda) + C_{CHL}\,a_{CHL}(\lambda) \qquad\qquad \text{EQ 1}$$
$$b(\lambda) = b_{water}(\lambda) + C_{SM}\,b_{SM}(\lambda) + C_{CHL}\,b_{CHL}(\lambda)$$

If the concentration levels are allowed to be user selectable and variable, the final step is to determine the optical cross sections, $a_{CDOM}(\lambda)$, $a_{SM}(\lambda)$, $a_{CHL}(\lambda)$, $b_{SM}(\lambda)$, and $b_{CHL}(\lambda)$. The literature contains several examples. The

particular water body in question normally has its own variety of chlorophyll-a and suspended matter so the optical cross sections are variable. Further, the values reported in the literature tend to range in wavelength from 400nm to 700nm because that is typically where water-viewing sensors operate. For the purposes in this study, data above 700nm and preferably in the range from 400nm to 1000nm are required. Bukata (1995) reports cross section curves for Lake Ontario waters in the 400nm to 690nm range and provides numerical equations for the key cross sections outside of that region. HydroMod uses Bukata's cross section data and equations as the default values and allows the user great flexibility to change these values. As part of this study and other ongoing work at RIT, the inherent optical properties (IOP's) specific to Lake Ontario and the waters feeding the Genesee embayment are being characterized through laboratory and field studies.

These data comprise most of the input to the HydroMod code to describe the water body. Other water parameters include internal sources such as bioluminescence, fluorescence, and Raman scattering. These sources are modeled in the original HYDROLIGHT code and modified in the HydroMod version of HYDROLIGHT, but they have not been emphasized on the first year of this study.

3 Multi-parameter Inversion Algorithm

A critical step in hyperspectral water quality assessment is the development of an inversion code that relates observed spectra to concentration values of the in-water constituents. In the previous section, we described a procedure for the forward modeling of reflectance spectra or sensor-reaching radiance based on IOP's, illumination, viewing conditions and constituent concentrations. If we convert the AVIRIS sensor-reaching spectral radiance values to surface reflectance spectra, we should be able to predict these spectra for a defined sensing scenario by just varying the constituent concentrations until a match is found. Given the range of constituent combinations and the number of spectral bands involved, this task requires some form of optimization algorithm.

3.1 Atmospheric Normalization/Correction

For this proof-of-concept study, we used a variation of a method suggested by Mustard (1999) to convert spectral radiance to surface spectral reflectance. In this method, clouds and cloud shadows are assigned reflectance values and a two point relationship between observed radiance and the assumed reflectance values is produced for each band. The scene can then be converted to spectral reflectance using a simple linear conversion for each band. This method has a tendency to introduce errors in the recovered reflectance of dark objects because the cloud shadows effective reflectance is difficult to estimate. An alternative dark pixel solution was employed involving selection of clear water points where we believed we could roughly estimate the constituent concentrations. In cases where ground truth is available this will be a very simple task (e.g., for the AVIRIS collects made as part of this effort over Lake Ontario). For these "known" clear water pixels the reflectance was predicted using the HydroMod routine based on the known or estimated constituent concentrations. The predicted reflectance spectrum was then used as the dark pixel in the empirical line method (ELM) radiance to reflectance conversion algorithm. This has two advantages. It removes atmospheric effects and compensates for any bias errors in the modeling process. Thus, the model only needs to correctly predict changes in reflectance to yield a good match with observations. Ongoing research is aimed at testing other algorithms that are designed for use in operational situations where ground truth is not available and/or where spatial atmospheric variability may be of concern.

3.2 Lookup Table Generation

Using the atmospheric correction algorithm described above, we can convert the image data to surface reflectance spectra. Given that the image data can now be expressed as reflectance spectra, we still need a way to optimize the inversion to multiple constituents. At this point, we have three parameters we wish to solve for [SM], [C] and [CDOM]. We can run the HydroMod code for the image acquisition conditions over a range of concentrations for each constituent and combinations of constituents. Each three parameter combination generates a reflectance spectrum characteristic of what a sensor should observe under those imaging conditions. We can assemble the output from many such runs into a three-dimensional lookup table (LUT) as illustrated in Figure 2. Each element in this LUT is a reflectance spectrum and can be accessed by the concentration values. Figure 3 shows several example spectra from the LUT. In order to estimate the spectrum of any combination of constituents
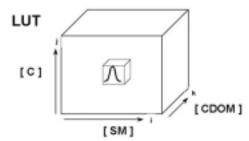
Figure 2 Multiparameter lookup table where each entry is a spectral vector.

not specifically in the LUT, we can perform a three-dimensional interpolation between the closest values.

We now have a three-dimensional LUT with a spectrum as each entry which is accessible by constituent. Our goal is to find the constituents associated with an observed spectrum for a particular pixel. To accomplish this we need a goodness of fit or error metric. The metric we used for this study is the squared error defined as

$$SE = \sum (R_{obs}(\lambda) - R_m(\lambda))^2$$

EQ. 2

where $R_{obs}(\lambda)$ is the observed reflectance at wavelength λ, $R_m(\lambda)$ is the corresponding modeled value and the sum is over the wavelength range of interest (in our case, we used values ranging from 420 nm – 680 nm). The wavelength range is chosen to take advantage of the bulk of the spectral range associated with coloring agents yet avoid fluorescence which may not yet be adequately modeled. Given this error metric, we seek to minimize the error when comparing the actual spectrum to those in the LUT or interpolated from LUT values. This is done with an optimization code.
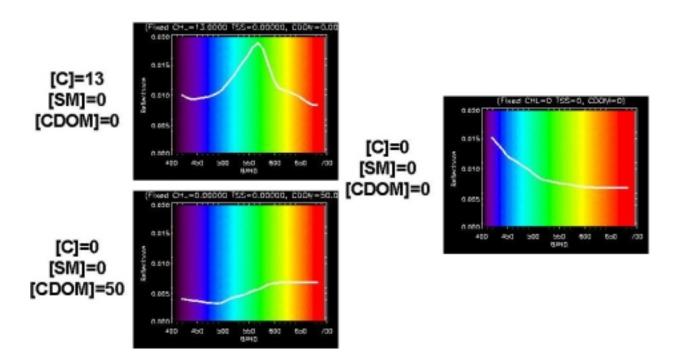

Figure 3 Example spectra for different entries in a LUT.

3.3 Optimization Algorithm

The optimization approach we implemented uses a downhill simplex algorithm sometimes called "AMOEBA"

(Press 1992). The method is most easily described in terms of a two-dimensional problem and then extended to multiple dimensions. In two dimensions, we would have two variables i and j that describe the indices to the LUT (these could also represent the actual constituent concentrations, but we will use the more generalized indexed approach). A simplex is formed in N-dimensional space by N+1 non-degenerate points (i.e., they span N dimensions). The algorithm starts by forming an arbitrary simplex in the i, j space of interest. The code is often initialized by locating the simplex close to the best guess at a solution. For example, in our case the solution for a previous pixel might be used. The simplex (i.e., the distance between points) is scaled to the estimated characteristic scale of the data set (e.g., 2 – 3 times the index values). The points in i, j space are evaluated in terms of their functional values and rank ordered from best (lowest) to worst (highest). The function for our work is the squared error between the spectrum of the pixel of interest and the spectrum accessed through the LUT for each vertex of the simplex in (i,j) space. The simplex then tries to expand and contract on the surface described by the squared error functional values in a fashion that progressively moves down hill until a minimum is achieved. This is accomplished through an iterative rule-based process.

In our case, the simplex exists in three dimensions and the final minimum value would occur at some non-integer point in our index space (l,m,n). We can then extract the appropriate concentrations using simple linear interpolation in each dimension. Figure 4 shows an example of an image-derived spectrum and the best-fit spectrum selected by the AMOEBA algorithm.
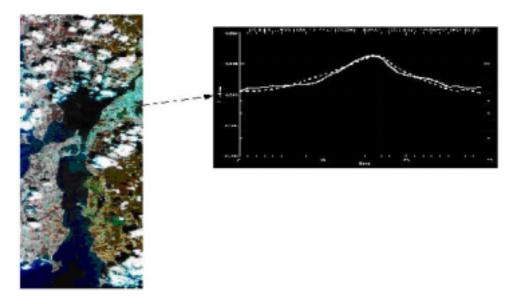

Figure 4 Illustration of an image derived reflectance spectrum (from the Narragansett Bay data) and the best fit spectrum selected by the AMOEBA optimization algorithm.
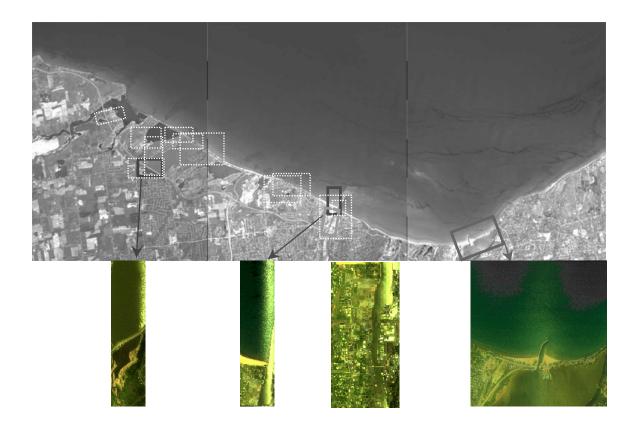
Figure 5 MISI flight coverage for AVIRIS collection date May 20, 1999 superimposed on partial AVIRIS browse image f990520t01p02_r03. The colored box outlines the MISI image of Irondequoit Bay. The white boxes outline other MISI data collected on this day.

4   Test Data

4.1   AVIRIS & MISI Collections Over Lake Ontario

On May 20, 1999, AVIRIS imaged two flight lines along the shores of Lake Ontario. In conjunction with this AVIRIS collect, RIT collected MISI (Modular Imaging Spectrometer Instrument) hyperspectral imagery (cf. Nordgren 1999) and launched an extensive field campaign to acquire ground truth. Figure 5 shows partial quick-look images from one of two flight lines with outlines showing corresponding MISI coverage acquired the same day at approximately the same time as the AVIRIS flight.

4.2   Ground Truth Data Collection

The ground collection involved, three boats (Boston Whaler in Lake Ontario or large bay, canoe and kayak in small bays), a radiometer pier/bridge team, deployment of truth panels, and two spectrometer teams. Water samples, secchi depths, and surface water temperatures were collected by each water team. Table 1 summarizes the equipment used for the ground truth data collection. The image and ground truth data are being integrated into RIT's Great Lakes Geographic Information System. This provides the ability to organize and analyze the data set in a unified system.

5   Results

5.1   Narragansett Bay Test Data

Because of delays in receiving the AVIRIS Lake Ontario data, the AVIRIS Narragansett Bay [August 19, 1997] data was used for initial testing of our algorithms. We would have preferred a data set with more turbid water and a good range of ground truth. However, since our early efforts were focused on data collection, product definition and tool development, we were able to effectively use the Narragansett data to evaluate trends in map products and major limitations. Detailed quantitative error analysis is a major focus of our ongoing efforts.

Our analysis of the Narragansett Bay data set concentrated on a flight line that covered the Sakonnet River. The first step in the analysis was to build a lookup table of reflectance spectra derived from the HydroMod model. Because our focus is the Great Lakes, we had concentrated on obtaining IOP's for the lakes and including them in HydroMod. The optical properties of Great Lakes and coastal waters should be similar but by no means identical. We would have liked to have run HydroMod with IOP's obtained from the waters under study. However, since these were not available, we proceeded using a LUT built using IOP's obtained from Dr. Robert Bukata (cf. Bukata et al. 1995). We expected that this LUT would be similar enough to the Narragansett coastal region to allow us to map patterns in the water. However, we do not expect to be able to quantify the parameters and may have problems in mapping even the spatial patterns of parameters with weak spectral structure (e.g., because of low concentration).

We began the analysis using a simple ELM based on clouds and cloud shadows. While this seemed promising, we quickly found we had improved performance using the model-based ELM where we generated the dark spectrum by assuming very low concentrations of constituents in the darkest ocean pixels in the scene. This dark reflectance spectrum was then used with a cloud spectrum assumed to be a 90% reflector to generate the ELM solution for radiance to reflectance calibration.

Table 1: Underflight and Ground Truth Instruments and Specifications

Instrument	Measurement	Specifications

RIT-Modular Imaging Spectrometer (MISI)
 	
    VNIR spectrometer
 	
    Thermal channels
	Calibrated image data with 4' to 20' GSD	2 milliradian IFOV,
		45 milliradian FOV,
		minimum flight altitude 2000'
		
		Range 0.4-1.0μm, 10 nm centers
		
		8-10μm, 0.5-11.5 μm, 2 @ 10-12.15 μm

ASD Field Spectrometer	Spectral reflectance/radiance	0.4μm-2.5μm
Photo Research 680	Spectral reflectance	0.4μm-0.8μm
2 Barnes PRT-5	Ground radiance or apparent temp.	3-5 or 8-12μm
Digital Camera (fisheye)	Sky radiance field	RGB channels
Everest IR thermometer	Apparent ground temperature	8-12μm
12 thermistors	Water temperature	
2 Garmin GPS	location	Positional accuracy 15m
2 ground truth panels	Reflectance target	10m x 10m
3 secchi disks	Secchi depth	8" disk, calibrated line
Shimadzu 2401PC spectrometer	Particle absorption and CDOM absorption	300-800nm
Hitachi spectrofluorometer	Chlorophyll a	Flurometric technique
Analytical balance	TSS (total suspended solids)	

The initial runs of the algorithm showed an inability of the HydroMod model to generate spectra in the lookup tables that were a good match to the brighter spectra in the AVIRIS image. This may in part be due to the use of the IOP's derived from Bukata et al's model-based derivation of IOP's. However, closer analysis pointed to an additional problem. This stems from the need to include an appropriate scattering phase function for suspended minerals in the HYDROLIGHT model. Because HYDROLIGHT has been primarily used for modeling deep ocean (Case I) waters, the scattering tends to be small with strong forward scattering. On the other hand, the scattering from suspended minerals is expected to have a much higher backscatter component. Thus, even if the correct spectral scattering cross section is used in HYDROLIGHT, the predicted reflectance spectra can be in error if the proper scattering phase function is not used. This has not been a major issue with researchers studying Case I waters, but is of critical concern for the more turbid Case II waters of interest on this project. The HYDROLIGHT code is capable of supporting a range of scattering phase functions. In interactions with Dr. Mobley, he indicates that the new version of HYDROLIGHT (4.1), which is under testing, has been upgraded to deal with this issue by allowing the user to control the backscatter coefficient input to the model. We expect to either implement similar changes to the HydroMod version of HYDROLIGHT or upgrade HydroMod to use HYDROLIGHT 4.1 when it is released. Given these limitations, we proceeded to apply the HydroMod data to the Sakonnet River data set where we did not expect to see very high [SM] values

Figure 6 shows chlorophyll and CDOM concentration maps for a long stretch of the Sakonnet River where it empties into the Ocean waters. The lookup table used to generate these data was produced using HydroMod with the IOP's from Bukata et al. 1995 updated with IOP's obtained from RIT field samples of the Great Lakes. The maps show encouraging results in terms of well-behaved patterns (i.e., consistent pixel-to-pixel results). We were also encouraged with the spatial patterns in the maps. The most obvious and intuitive result is the significant reduction in the concentration of constituents where they are diluted by the ocean waters. There is also a significant line of increased CDOM running roughly perpendicular to shore in the coastal waters. This transition line can be seen by contrast stretching the raw data and appears to be associated with discharges further along the coast to the right (outside the image). If we look up the river, we see that the chlorophyll concentrations appear to increase around nutrient sources associated with the major inflows. We also see a tendency for the CDOM concentrations to be somewhat correlated with chlorophyll. However, we also see several small localized increases in CDOM along the river bank often associated with drainage sites where we would expect CDOM to increase. We were also encouraged that there is some decorrelation between the maps indicating that we are separating out spectral structure and not simply tracking brightness variations. The only obvious failure of the process was the regions of localized high CDOM (burgundy and red areas) surrounded by low CDOM (blue area) at the bottom of Figure 6. These areas which go from very low to very high with no gradation are suspect. We believe this is a result of stray solutions in the optimization routine that occur for very dark water pixels (darker than we expect in the Great Lakes). We believe that these stray solutions can be eliminated with error trapping.

It is important to note at this point that the range of sampled data from the Lake Ontario field collection is typically four times the total range spectral in Narragansett Bay. This is very encouraging because the more variation in the data, the more range over which the models have to operate and the more likely we are to be able to track significant variations in materials (i.e., all the action is not down in the noise).

The focus of ongoing work is to produce an initial quantitative analysis of the Lake Ontario data set and to improve the inputs to the HYDROLIGHT routine to more appropriately model the higher scattering levels associated with the Case II waters that are the target of this study.
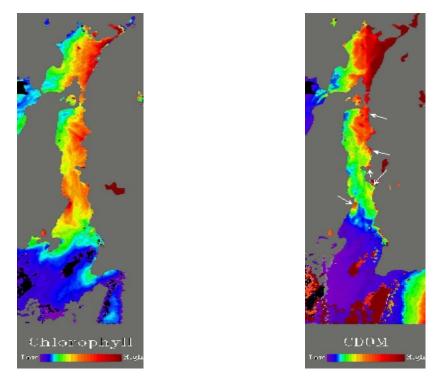
Figure 6 Chlorophyll CDOM concentration map produced using the HydroMod LUT.

6   References

Berk, A., L.S Bernstein., & D.C Robertson., 'MODTRAN: a moderate resolution model for LOWTRAN 7, GL-TR-89-0122 Spectral Science, Burlington, MA 1989.

Bukata, Robert P., John H. Jerome, Kirill Ya. Kondratyev, and Dimitry V. Pozdnyakov, "*Optical Properties and Remote Sensing of Inland and Coastal Waters*", New York: CRC Press, ISBN 0-8493-4754-8, 362 pages, 1995.

Cox, Charles and Walter Munk, "Slopes of the Sea Surface Deduced from Photographs of Sun Glitter", *Bulletin Scripps Institute of Oceanography of the University of California*, Vol. 6, No. 6, pp. 401-488, 1956.

Fairbanks, R.R., J.R. Schott, N.G. Raqueno, R.E. Simmons, "Water quality monitoring with HSI," presented at ISSR Systems and Sensors for the New Milennium, Las Vegas, October 1999.

Green, R. O., Roberts, D. A., Conel, J. E., "Estimation of aerosol optical depth, pressure elevation, water vapor and calculation of apparent surface reflectance from radiance measured by the airbourne visible/infrared imaging spectrometer using a radiative transfer code," SPIE Vol. 1937, Imaging Spectrometry of the Terrestrial Environment, pp. 2-11, (1993).

Mobley, Curtis D. "*Light and Water: Radiative Transfer in Natural Waters*", Boston, Academic Press, ISBN 0-12-502750-8, 592 pages, 1994.

Mobley, Curtis D. "*HYDROLIGHT 3.0 User's Guide*", SRI International, SRI Project Number 5632 Final Report, Office of Naval Research Contract number N00014-94-C-0062, Menlo Park, CA, 65 pages, March 1995.

Mobley, Curtis D. "*HYDROLIGHT 3.1 User's Guide*", SRI International, SRI Project Number 6583 Final Report, Office of Naval Research Contract number N00014-95-C-0238, Menlo Park, CA, 65 pages, April 1996.

Mustard, J.F., M.L. Staid and W. Fripp, "Atmospheric correction and inverse modeling of AVIRIS data to obtain water constituent abundances," Proceedings of NASA, JPL, AVIRIS Workshop 1999.

Press, W.H., *Numerical Recipes in C: The Art of Scientific Computing*, pp. 408-412, Cambridge University Press, 1992.

Sanders, L.C., R.V. Raqueño, and J.R. Schott, "An atmospheric correction algorithm for hyperspectral imagery," SPIE Europto, Florence, Italy, September 1999.

Schott, J.R., T. Gallagher, B. Nordgren, L. Sanders, .J. Barsi, "Radiometric calibration procedures and performance for the Modular Imaging Spectrometer Instrument (MISI)." Proceedings of the Earth Intl. Airborne Remote Sensing Conference, ERIM, 1999